Supplementary material

1. Geology

The geological study of the MW site complex focused on the petrogenesis of the felsic pyroclastic rocks and their depositional and geomorphic history as well as the associated volcano-clastic and fluvio-lacustrine sediments. Resom et al. (2018) conducted detailed field stratigraphic characterization (Supplementary figure 1.1) in combination with petrographic and whole rock major and trace element geochemistry. The results of these studies were used to correlate rocks and sediments across the MW site complex as well as in archaeological discussion of availability, procurement and transport of raw materials for the production of lithic assemblages. In the Upstream sector, the following major volcanic and sedimentary units were identified: (a) unwelded tuff; (b) welded tuff; (c) intercalated conglomerate and sand, with thin ash fall and units of ash flow interspersed in the sediments; (d) fractured, crystalline ignimbrite; (e) gray ash fall; (f) pumaceous ash fall; and (g) moderately welded, crystalline ignimbrite (Supplementary figure 1.2). The Downstream sector is dominated by a single major unit, a gray to bluish vitric and lapilli ash flow, with ash fall intercalations (Supplementary figure 1.2).

Due to the discontinuous nature of the deposits, stratigraphy has been studied across the site at logging locations in the Upstream and Downstream sections of the site. Logs in each sector (9 and 8 logs, respectively, in the Upstream and Downstream sections) were located at ~10-20 m lateral distance from each other (Supplementary figures 1.1-1.2) and were *intra*-correlated within section. The archaeological localities were incorporated into these two stratigraphic schemes.

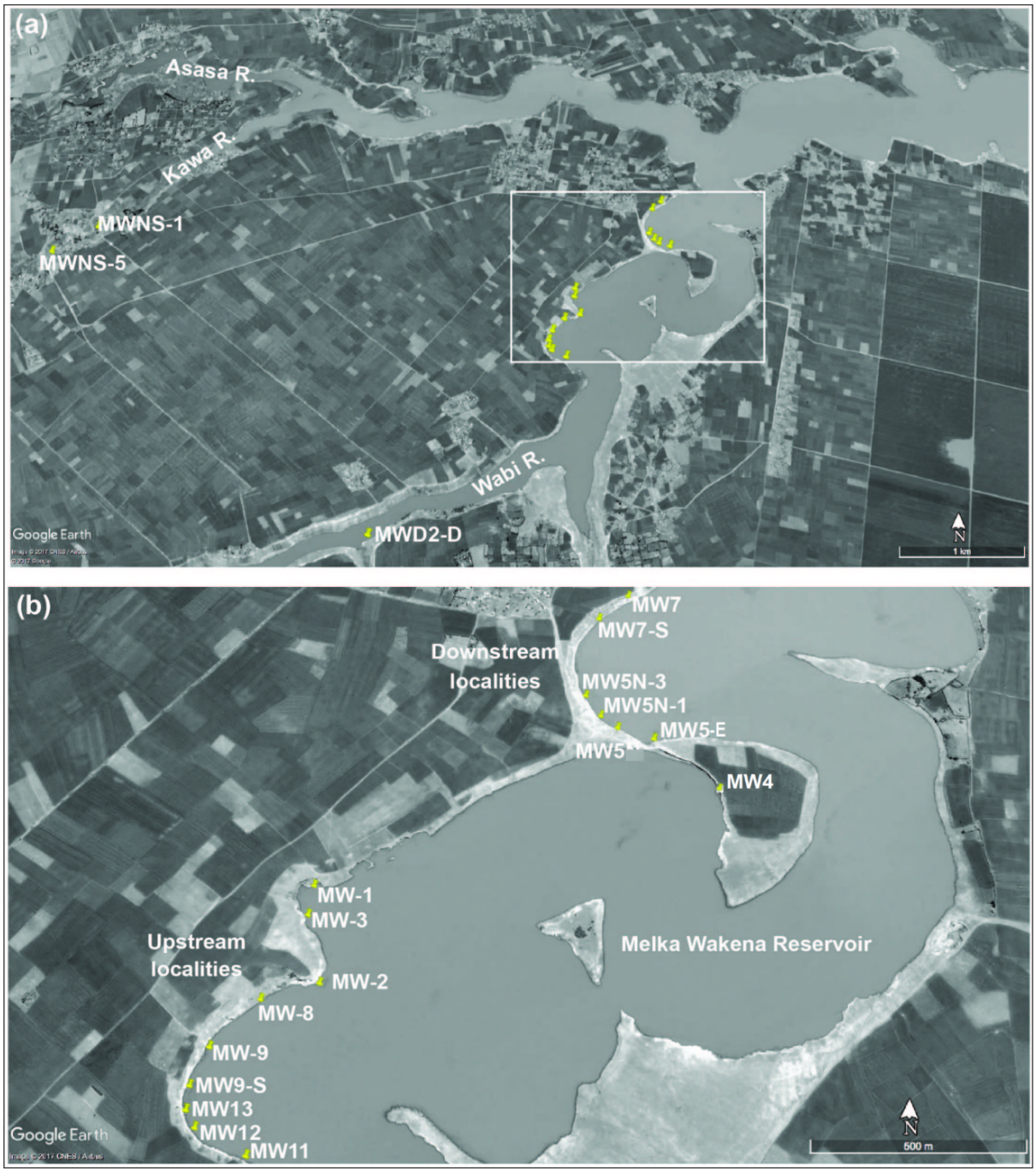

Supplementary Figure 1.1: Top: Aerial view of the Melka Wakena area, showing geological sampling locations outside the area of the site complex. Bottom: Closer view of the MW site-complex area. Logging and sampling locations along the Wabe River are indicated (Modified from Resom et al. 2018).

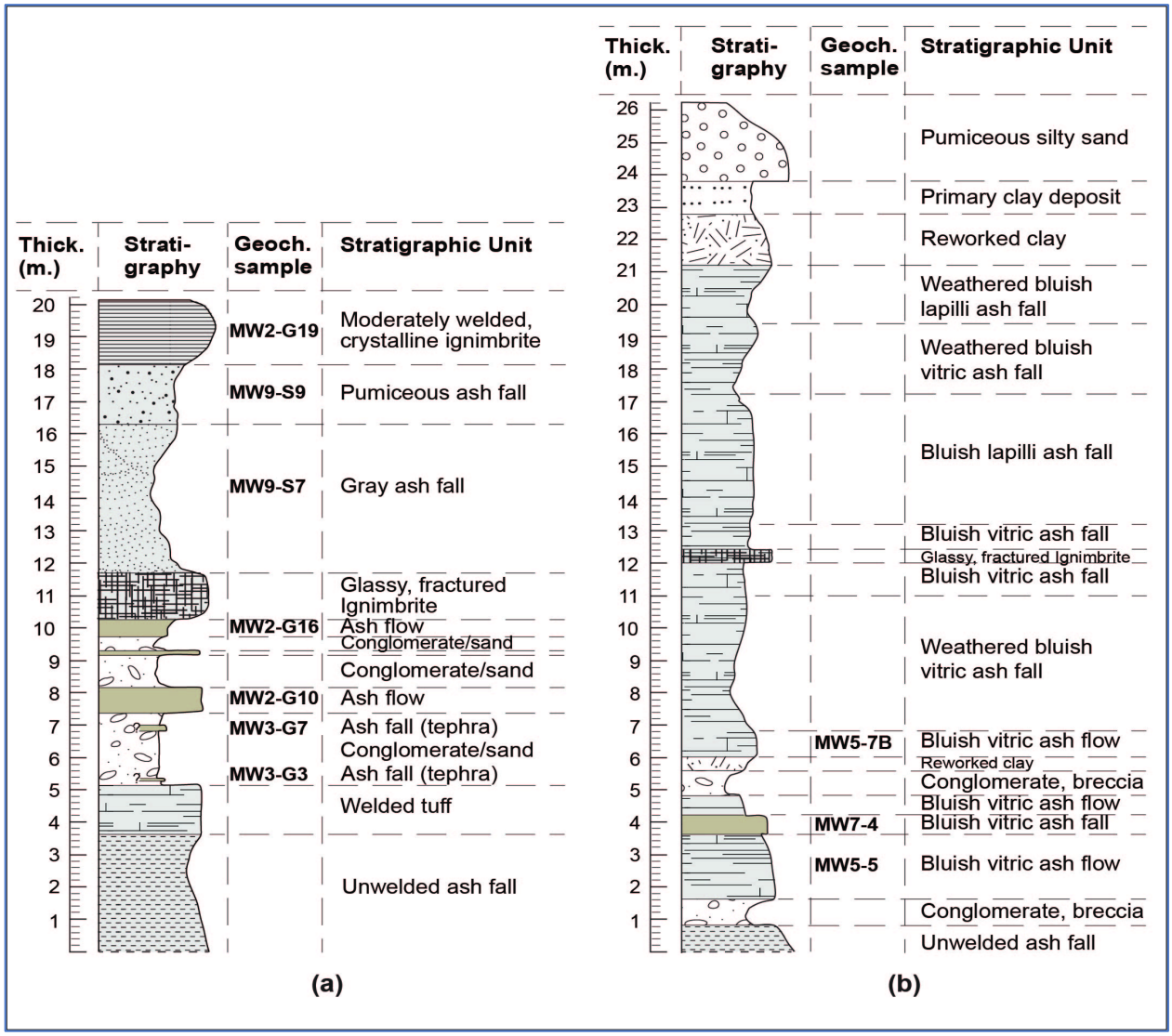

Supplementary Figure 1.2: Composite stratigraphic columns of the Upstream (a) and Downstream (b) sections at the MW site.

2. $^{40}Ar/^{39}Ar$ geochronology

Samples were sieved and washed in distilled water in an ultrasonic bath. Sanidine crystals were separated using a Frantz Isodynamic magnetic separator and heavy liquids. All samples were finally handpicked to purity. Sanidines were loaded into pits in 18.5-mm Al-discs with Alder Creek sanidine (ACs) in alternating pits to be used as neutron fluence monitors. The Al-discs were assigned irradiation numbers 458PRA and 469PRB from two different collection years and irradiations. One set of samples was irradiated for 2 hours (458PRA) and the other for 1 hour (469PRB) at the Cd-lined, in-core CLICIT facility of the Oregon State University TRIGA reactor. All samples, including ACs standards, were analyzed on MAP mass spectrometers; samples from irradiation #458PRA were analyzed on the MAP 215-50 instrument

dubbed Nexus, and those from #469PRB were analysed on the MAP 215-C instrument dubbed MAP 1. Both mass spectrometers have a Nier-type ion source and analogue electron multiplier detectors. Single grains of MW samples underwent total laser fusion from a CO_2 laser at 7 Watts of power. ACs samples from small pits were measured by total fusion of 3-grain aliquots. For each sample, blank and air pipette, fifteen cycles were determined for each Ar isotope using peak hopping by magnetic field switching on a single detector. Evolved gases were cooled to ca. -100 to -135 °C using a cryotrap and exposed to a c. 450 °C hot getter to remove condensable and reactive gases. For all samples, a mean blank correction was determined using background isotopic measurements analyzed between each single-grain analysis. Blanks between sample measurements were stationary over time, and mean values and standard deviations of blanks through the run were used to correct the sample and air pipette data. Mass discrimination was determined based on automated analyses of air pipettes between every five single grain analyses (plus intercalated blanks) using air pipette data based on a power law correction (Renne et al., 2009) and the atmospheric values of Lee et al. (2006). See the data in Supplementary Table 1 for mass discrimination values. All age uncertainties, as well as uncertainties in Ar isotopes, are reported at the level of 1σ here and throughout. Interference corrections were based on the following nucleogenic production ratios (Renne et al., 2015): $(^{40}Ar/^{39}Ar)_K = (7.30 \pm 0.92) \times 10^{-4}$; $(^{38}Ar/^{39}Ar)_K = (1.196 \pm 0.013) \times 10^{-2}$; $(^{39}Ar/^{37}Ar)_{Ca} = (7.02 \pm 0.12) \times 10^{-4}$; $(^{37}Ar/^{39}Ar)_K = (2.24 \pm 0.15) \times 10^{-4}$; $(^{36}Ar/^{37}Ar)_{Ca} = (2.702 \pm 0.004) \times 10^{-4}$; $^{36}Cl/^{38}Cl = (2.628 \pm 0.002) \times 10^{-3}$. Total fusion results of ACs were used to calculate J values and provide the basis for liner interpolation of J values for unknowns. J values of Melka Wakena samples were determined by interpolation of a planar fit to J-values determined from the ACs fluence monitor (ACs monitor age = 1.1891 ± 0.0008 Ma; Niespolo et al., 2017; Renne et al., 2011). Ages were calculated using the calibration of Renne et al. (2011).

Supplementary table 2.2: Ages and duration of Marine Isotope stages (MIS) associated with Highland archaeological localities

Locality	Bracketing mean ages (Ma)	MIS
MW2-L4, MW2-L3,	1.622-1.445	56 - 48
MW5-L3	1.626-1.370	56-44
MW2-L2	1.445-1.340	48-43
MW5-L1	1.370-1.340	45-43
MW2-L1	1.340-1.224	45-38
Garba IVD	1.719-1.429	62-48
Garba XIIIb	1.037-0.869	31-23

*Localities and archaeological ages from this paper, Gallotti and Mussi (2017); MIS numbers from Lisiecki and Raymo (2005)

3. Excavation

MW2 and MW5

Four distinct archaeological layers, designated independently of geological units, were identified (Figure 4, main text) in the sequence of MW2 locality and numbered as layers 1-4 (top to bottom). Layers MW2-1 and MW2-2 were heavily disturbed by commecrcial sand quarring acitvities and could not be excavated systematically. Remnants of the *in situ* horizons were identified some 10 m to the east and verified as the stratigrpahic origins of stone artifacts scattered along a relatively gentle slope above the *in situ* Layers 3 and 4. All the visible items assigned to these layers were collected from an area of 20 m^2 on the slope and were attributed to "Layers 1&2" without further distinction.

A virtual site-specific 1x1 m grid system was set in order to facilitate monitoring the progress of field workers and to provide context for items retrieved in the sieve. Three-dimensional coordinates were obtained for each visible find encountered during excavation, using a Sokkia 630 total station (TS). Detailed maps of all finds and excavation profiles were drawn at a scale of 1:10. Twelve measurements with a hand-held GPS to known points in the site were later used to geo-reference the

locality and the finds, and all maps and profile drawings were digitized (e.g., Figure 5; Supplementary fig. 3.1).

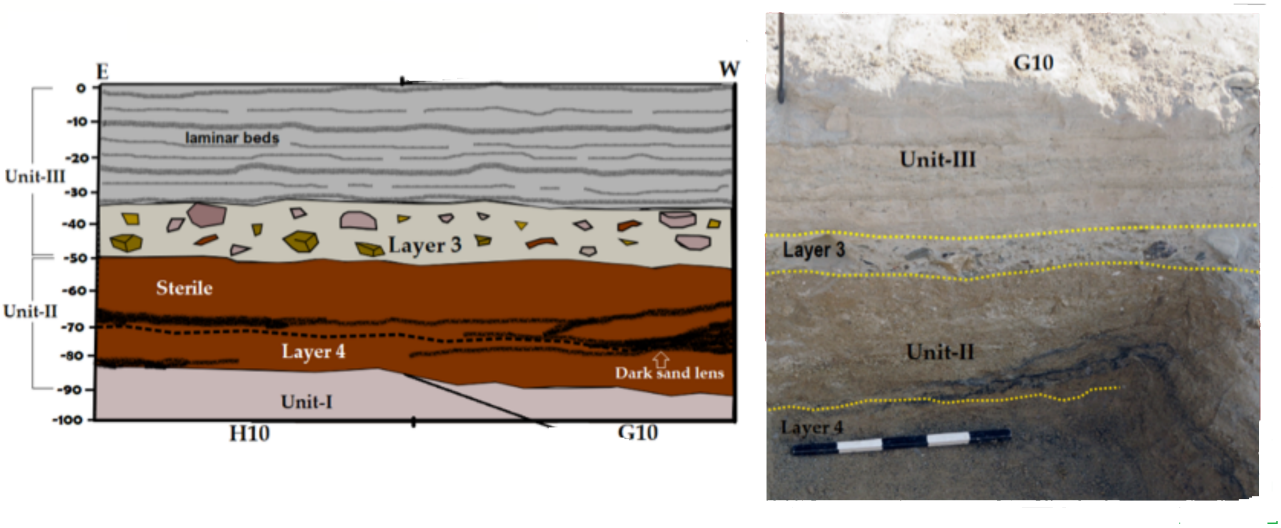

***Supplementary figure 3.1*:** Schematic rendering (left) and photograph (right) of the south-east profile at MW2, showing the relationship between the geological units and the archaeological layers MW2-L3 and MW2-L4

Sediments were removed according to grid square and 10-cm elevation spits and sieved through a 5-mm mesh. This allowed attribution of items retrieved in the sieve to specific spatial and stratigraphic context.

Excavations at MW5 followed the same procedures, except that maps and sections were drawn using a Leica FlexLine TS06 rather than manually (e.g., Figure 7 Supplementary figures 3.3-3.4).

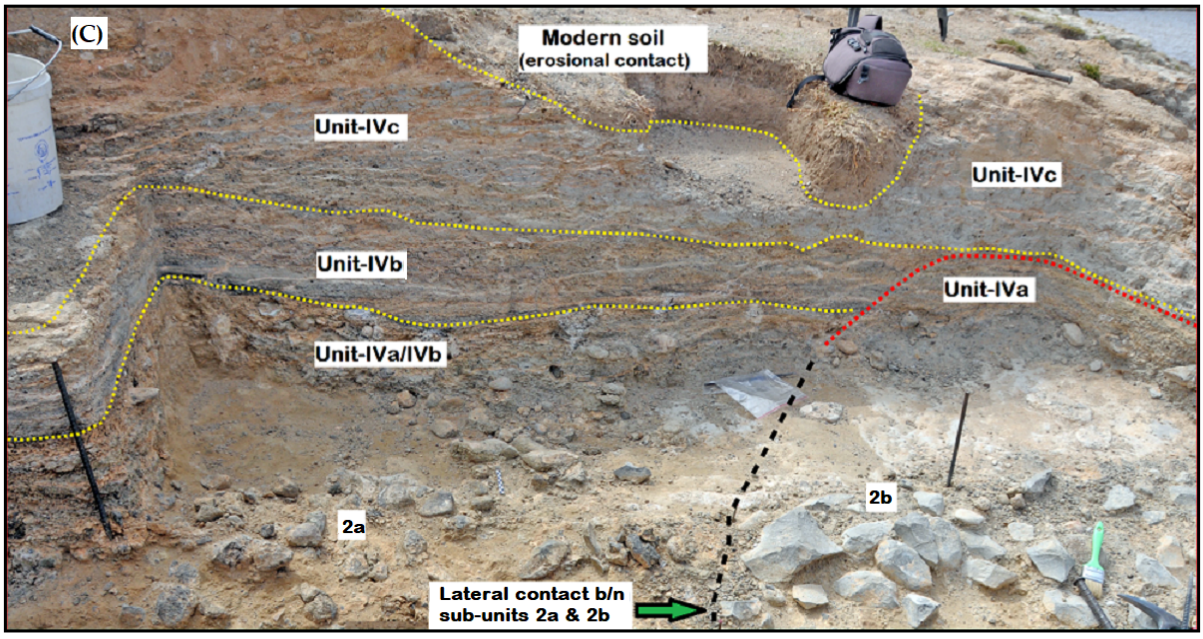

Supplementary figure 3.2: View of sub-units of Unit IV in the western part of the excavation at MW5. Dotted lines in yellow demarcate sub-units within Unit IV on the western excavation profile. Note the lateral contact between sub-units IVa & IVb (marked by the dashed black line, denser where the contact is observed in section) and the differences in artifact appearance on the two sides of the suggested contact.

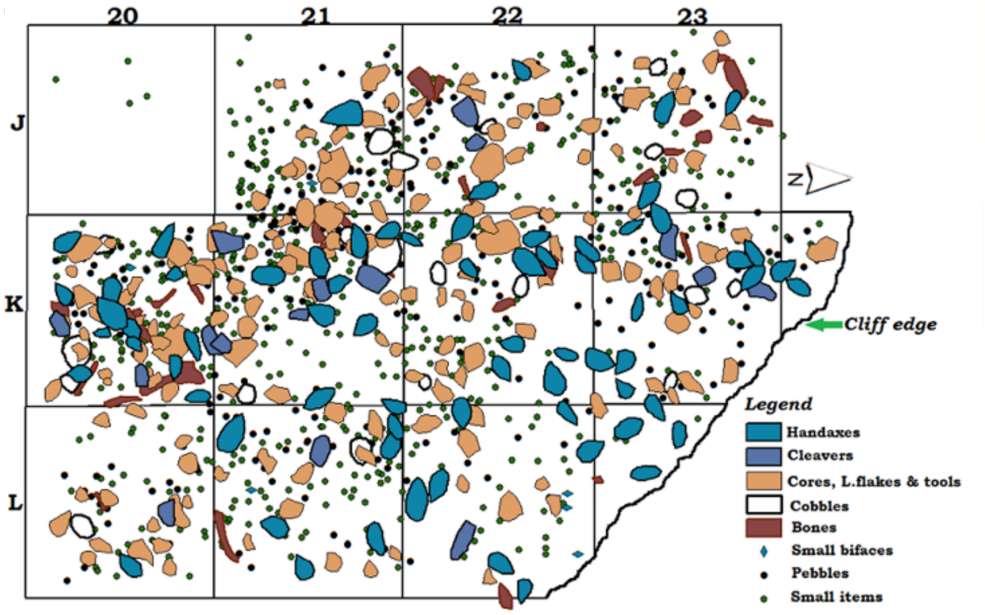

***Supplementary figure 3.3*:** Georeferenced distribution map of all the piece-plotted items in MW5-L2 and MW-L1. Grid squares are 1x1 m.

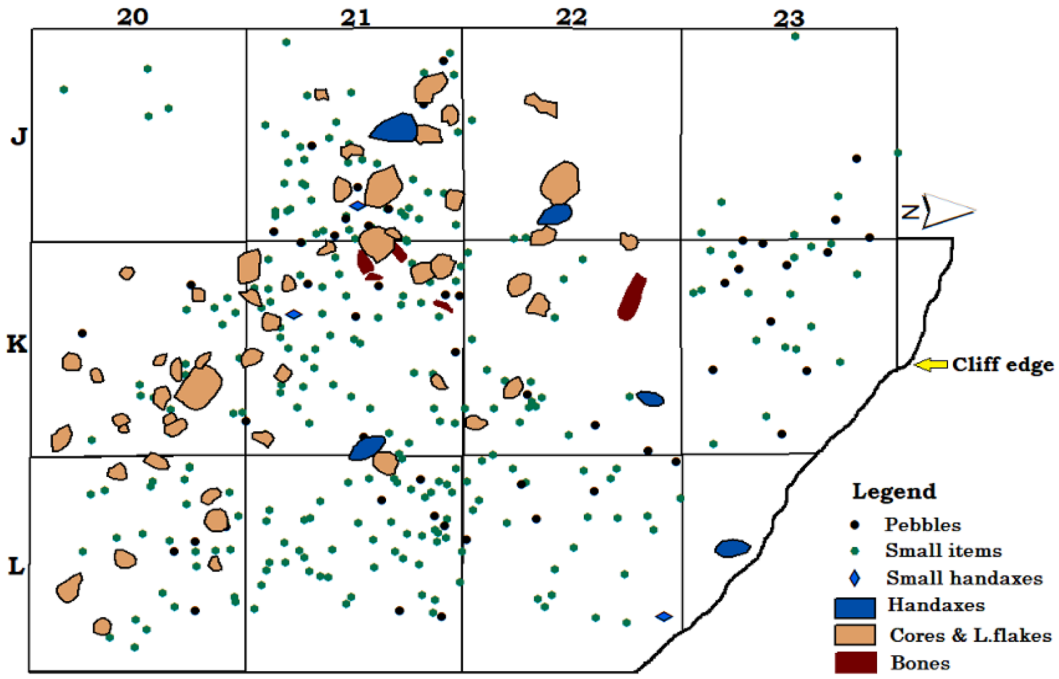

***Supplementary figure 3.4*:** Georeferenced distribution map of piece plotted items in MW5-L1. Grid squares are 1x1 m. See Figure 7 in main text for maps of MW5-L2 facies.

MW1

Eroded artifacts were exposed at lower topographic elevation along the shoreline, due to receding lake levels. These were mapped schematically in order to document their spatial relation to one another and then collected individually. This collection was designated MW1-surface. Field observations indicated that several artifact-bearing levels, identified as discontinuous horizons at various elevations may have contributed to this collection. Given the considerable overburden of some 1.5 m of recent soil and post-archaeology deposition, a step trench was dug in order to examine the presence of such horizons and their stratigraphic relationship. Steps were cut 2 m across, 0.5 m high and 0.5 m deep, and were numbered consecutively from top to bottom. Steps 1 and 2 did not reveal any finds, whereas steps 3 and 4 each contained dense artifact concentrations. All finds were collected systematically but without detailed mapping of individual items and assigned to the step of origins (S-3 or S-4). Sediments were dry sieved through a 5 mm mesh and the retrieved finds were assigned to a step.

4. Paleontology

The current vertebrate faunal list from across the Melka Wakena site is composed of 15 species of large vertebrates (*Crocodylus* cf. *niloticus*, and 14 mammals), originating from the stratigraphic sections in the excavated MW localities and from extension of correlated stratigraphic layers across the site.

Abbreviations of measurements: Measurements: L: length; W: width; WAL: width anterior lobe; WPL: width posterior lobe; Lprt: length protocone; prt index: protocone index; APD: antero-posterior diameter; MLD: medio-lateral diameter; PMLD: proximal medio-lateral diameter; PDVD: proximal dorso-ventral diameter; MMLD: medial medio-lateral diameter; MDVD: medial dorso-ventral diameter; DMLD: Distal medio-lateral diameter; DDVD: distal dorso-ventral diameter; ML: medial length; LL: lateral length; CL: Central length .

Systematic paleontology

Class Reptilia Laurenti, 1768
Order Crocodylia Gmelin, 1788
Family Crocodylidae Cuvier, 1807
Genus *Crocodylus* Laurenti, 1764
Species *Crocodylus* cf. *niloticus* (Laurenti, 1768)

Material: #MW5-B62: 1 fragment of left femur coming from MW5 (Supplementary figure 4.1) and some undetermined bone fragments from area MW4.

Description: #MW5-B62 is a proximal part of the femur diaphysis without medullary cavity and compact tissue. The MMLD is 23.98 mm and the MDVD is 24.94, corresponding to a juvenile individual.

Supplementary Figure 4.1. Left femur B62 from MW5 of *Crocodylus* cf. *niloticus*. A) dorsal view; B) medial view; C) ventral view; D) lateral view.

Class Mammalia Linnaeus, 1758
Order Rodentia Bowdich, 1821
Family Hyxtricidae Burnett, 1830
Genus *Hystrix* Linnaeus, 1758
Species *Hystrix* sp.

Material: 1 incisor from MW1.

Description: A nearly complete middle size incisor of a porcupine.

Class Mammalia Linnaeus, 1758
Order Carnivora Bowditch, 1821
Family Canidae Fischer von Waldheim, 1817
Subfamily Caninae Fischer von Waldheim, 1817
Tribe Canini Fischer vonWaldheim, 1817
Genus Cf. *Canis* Linnaeus, 1758
Species Cf. *Canis* sp.

Material: A mandibular fragment from MW5- unit II.

Description: An elongated mandibular fragment of an indeterminate small size canid.

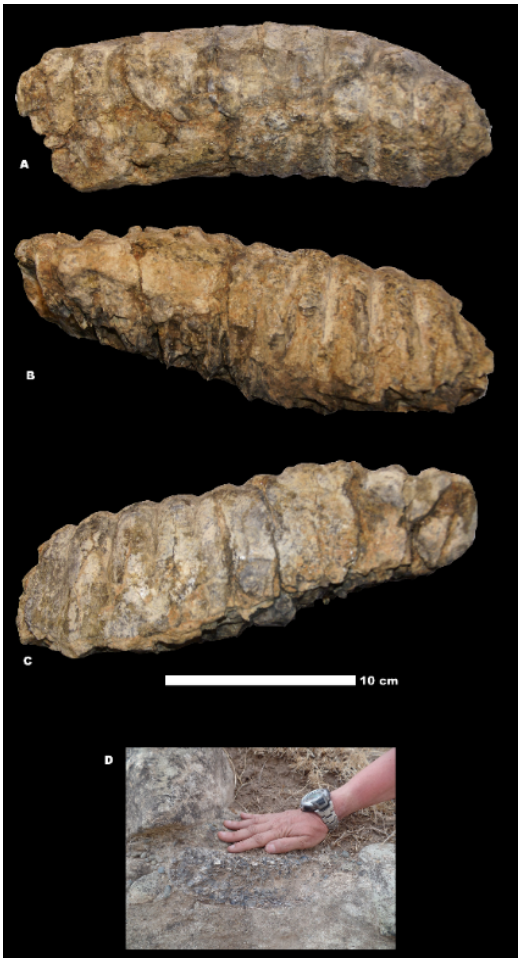

Order Proboscidea Illiger, 1811
Family Elephantidae Gray, 1821
Genus *Elephas* Linnaeus, 1758
Species *Elephas recki* (Dietrich, 1894)
Subspecies *Elephas recki* cf. *brumpti* Beden, 1980

Material: A lower left m3 from MW7 (Supplementary table 4.1 Supplementary figure 4.2).

Description: 1 lower 3rd molar of a very young adult individual (age at death ~20 years). It has a very low crown, thick enamel (4.00-4.70 mm) and a low frequency of plates (5 per 10 cm).

Supplementary figure 4.2. Left lower m3 of *Elephas recki* cf. *brumpti* from MW7. A) occlusal view; B) labial view; C) lingual view; D) Specimen in situ showing the base of the teeth without roots.

Supplementary Table 4.1: Measurements of the tooth specimen from the MW7 ascribed to *Elephas recki* cf. *brumpti.*

Elephas recki* cf. *brumpti, *lower 3rd molar*	
Total Length	*235.0 mm*
Occlusal Length	*88.24 mm*
Maximum Width	*79.43 mm*
Maximum Height of the tooth	*73.18 mm*
Number of plates	*10*
Functional plates	*3 (partially worn)*
Plate frequency per 10 cm	*5*
Enamel thickness	*4.00-4.70 mm*

Discussion: This molar corresponds to the lineage of elephants recorded in the African Plio-Pleistocene ascribed to *Elephas recki.* Several authors include these forms of elephants in the genus *Palaeoloxodon* Matsumoto, 1924 (see Lister, 2015, and references therein).

During the Pliocene and early Pleistocene, the lineage presents a trend of increase in hypsodonty, increase in plate frequency, and decrease of enamel thickness (related with the increase of plate frequency; Ferretti et al., 2003). This evolution is paralleled in other lineages of modern elephants, such the genus *Mammuthus* in Eurasia, with a succession of species adapted to colder, open and dry environments.

This tooth was located just on top of a silty volcanic ash and below the ignimbrite boulders at the section of MW7, younger than 1.3 Ma. The anatomical characteristics and metric data of this specimen preclude its inclusion in the Pleistocene species of this age, *E. recki recki*. Examination of the depositional context confirmed that this tooth was found in a channel filled by coarse-grained conglomerate (ignimbrites, and some basalts set in possibly fine grained ash matrix). Most likely it was reworked from a Pliocene stratigraphic series (though the potential geographic source cannot be accurately defined, the Mio-Pliocene Nazareth Formation which occupies the older sequences of the Assasa-Gadeb plain, which also possibly contained some sedimentary sequences intercalated with the volcanic formation, is a likely source).

Order Perissodactyla Owen, 1848
Family Equidae Gray, 1821
Genus *Equus* Linnaeus, 1758
Species *Equus* sp.

Material: 1 left upper 4th premolar (P4) from MW4 (stratigraphically equivalent to MW2-L1&L2); 1 right 4th metatarsal from MW4; 1 fragmented left upper premolar (from N 0704827, E 3915666); 1 complete left upper 2nd molar (MW2) (from N 0709814, E 3915657); ½ proximal left tibia from MW4; 1 right lower dp3-dp4 from MW5-L2b; #MW5-B177: 1 upper right molar or premolar of middle size from MW5-L2a); #MW5-B138: 1 upper left M3 from MW5-L2b).

Description: Four teeth were collected *in situ*. The specimens correspond to a middle size horse (Supplementary table 4.2). The upper molars have large protocones with a high protocone index, especially developed in the molars (66.82); the caballine fold is small and present at the 4th P but it is vestigial in the 2nd M; the fossetta plications

are simple (Supplementary figure 4.3). The unnumbered right lower deciduous premolar dp3-dp4 MW5-K22 corresponds to a small-middle size *Equus*.

Supplementary Table 4.2: Measurements of the *Equus* sp. teeth from MW.

***Equus* sp. ,** *dentition*				
	L	Lprt	prt index	w
Left upper P4 (MW4)	*21.70*	*10.80*	*49.77*	*24.52*
Left upper M2 (MW2)	*21.31*	*14.24*	*66.82*	*22.77*
Left upper P3-4 (MW8)				*24.89*
	L	*WAL*	*WPL*	*Preserved Crown Height*
Dp3-4 MW5-L3b	*27.78*	*9.99*	*9.64*	*21.78*

Discussion: All the specimens correspond to a small-middle size species of the genus *Equus* (i. ex. from the later Omo Beds: Churcher and Hooijer, 1980), and their anatomy is close to the open savanna zebra *Equus grevyi*.

***Supplementary figure 4.3*:** Upper left M2 of *Equus sp.* A) occlusal view; B) lingual view; C) distal view; D) labial view; and E) mesial view. Scale bar: 5 cm.

Order Artiodactyla Owen, 1848
Suborder Suina Gray, 1821
Family Suidae Gray, 1821
Genus *Metridiochoerus* Hopwood, 1926
Species *Metridiochoerus modestus* (Van Hoepen and Van Hoepen, 1932)

Material: 2 lower m3, left and right, probably corresponding to a single individual, from MW5-Unit II (Supplementary figure 4.4); #MW5-B45:3 rd molar fragment from MW5-L2b; 1 unnumbered molar fragment from MW5-L2b, corresponding to a third molar (Supplementary table 4.3).

Description: The best-preserved specimens, two lower m3, left and right, respectively, from MW5-Unit II, correspond to a form of the known small size species of the genus *Metridiochoerus*, *M. modestus*. These specimens have enamel in the labial, lingual, mesial and distal surfaces. Protoconid and metaconid are separated by a pair of central tubercles from hypoconid and entoconid, and more central tubercles separate these cusps from the talonid. The enamel corrugation is marked and present along the teeth.

Supplementary Table 4.3. Measurements of the teeth specimens ascribed to *Metridiochoerus modestus* from MW, compared with those from Buia, Eritrea (Martínez-Navarro et al., 2004).

Metridiochoerus modestus, *M3*			
MW	L	W	enamel thickness
MW5-Unit II, left	*55.62*	*11.80*	*1.19*
MW5-Unit II, right		*11.94*	
MW5-B45		*10.49*	
BUIA (Eritrea)			
UA-449	*45.1*	*13.5*	
DAN-220 R.	*42.2*	*14.4*	

Supplementary Figure 4.4: Left (complete) and right (incomplete) lower m3s of *Metridiochoerus modestus* coming from MW5-Unit II. A) occlusal view; B) labial view; and C) lingual view.

Discussion: These specimens correspond to *Metridiochoerus modestus*, the small size species of *Metridichoerus* (see Harris and White, 1979), which is well recorded in the later part of early Pleistocene of eastern and northern Africa.

Family Hippopotamidae Gray, 1821
Genus *Hippopotamus* Linnaeus, 1758
Species *Hippopotamus gorgops* Dietrich (1926)

Material: 1 Left lower canine (N 0704804 E 3916394); #MW2-B898: First premolar fragment (MW2-L3); 1 Pelvis fragment; #MW2-B927: Cervical vertebra (both from MW2-L4); #MW2-B929: medial tibia fragment (MW2-L3); #MW2-B932: right talus (lateral extension of MW2-L3; N 0704860, E 3915775) (Supplementary figure 4.5, left); #MW2-B933: left talus (lateral extension of MW2-L3; N 0704863, E 3915778) (Supplementary figure 4.5, right); #MW2-B878: Distal end of right tibia (MW2-L4; Supplementary figure 4.6); right IV metatarsal, partially destroyed in its proximal end(MW4); hemimandible of juvenile individual partially destroyed (MW6; N 0705583, E 3916326); upper canine, not well preserved (MW6; N 0705581, E 3916364); #MW5-B135: lower central incisor (MW5-L2b); #MW5-B66: two germinal lobes, mesial and distal, of an upper M3 (MW5-L2b); unnumbered specimen (found on

15/02/2017), corresponding to an upper left M1 (MW5-L2a/b); (Supplementary table 4.4).

Supplementary Table 4.4. Measurements of the specimens ascribed to *Hippopotamus gorgops.*

Hippopotamus gorgops		
DENTITION	*MW 5 n/n upper M3*	*#MW5- B135 low cervical incisor*
L	41.27	>175.67
WAL	33.03	
WPL	32.91	
DDV		38.70
MLD		36.85
TALUS	*#MW2-B932*	*#MW2-B933*
PMLD	*101.72*	*85.28*
DMLD	*96.16*	*87.72*
DDVD	*73.64*	*59.29*
ML	*104.50*	*89.65*
LL	*124.07*	*99.60*
CL	*112.40*	*93.02*
TIBIA	*#MW2-B878*	
DMLD (max.)	*101.80*	
DMLD (art.)	*92.79*	
DDVD	*76.52*	
IV METATARSAL	*MW4*	
L	*139.25*	
PDVD		
MDVD	*23.72*	
MMLD	*41.03*	
DDVD	*44.83*	
DMLD	*39.27*	

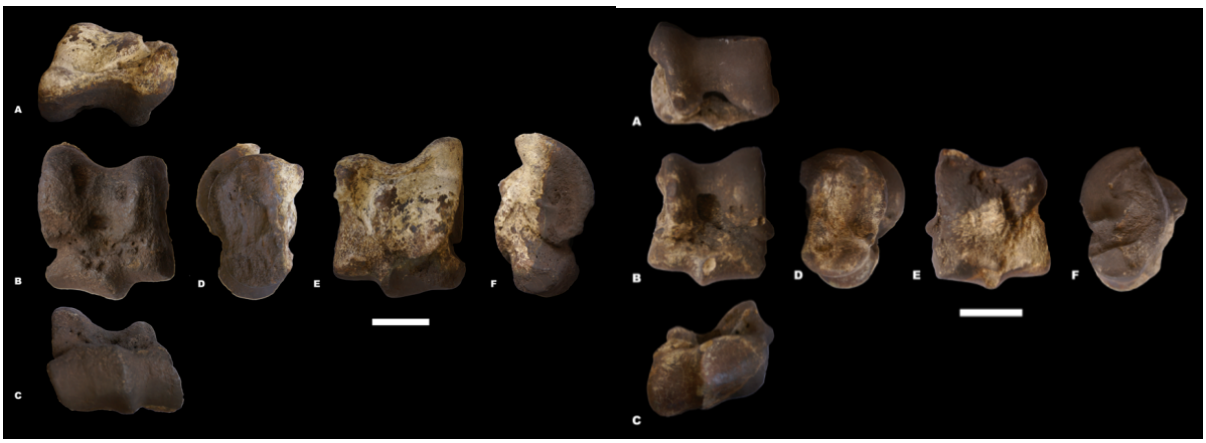

Supplementary Figure 4.5: Specimens #MW2-B932 (left) #MW2-B933 (right), right and left talus of a male and a female, respectively of *Hippopotamus gorgops*. A) proximal view; B) dorsal view; C) distal view; D) medial view; E) ventral view; F) lateral view. Scale bar: 5 cm.

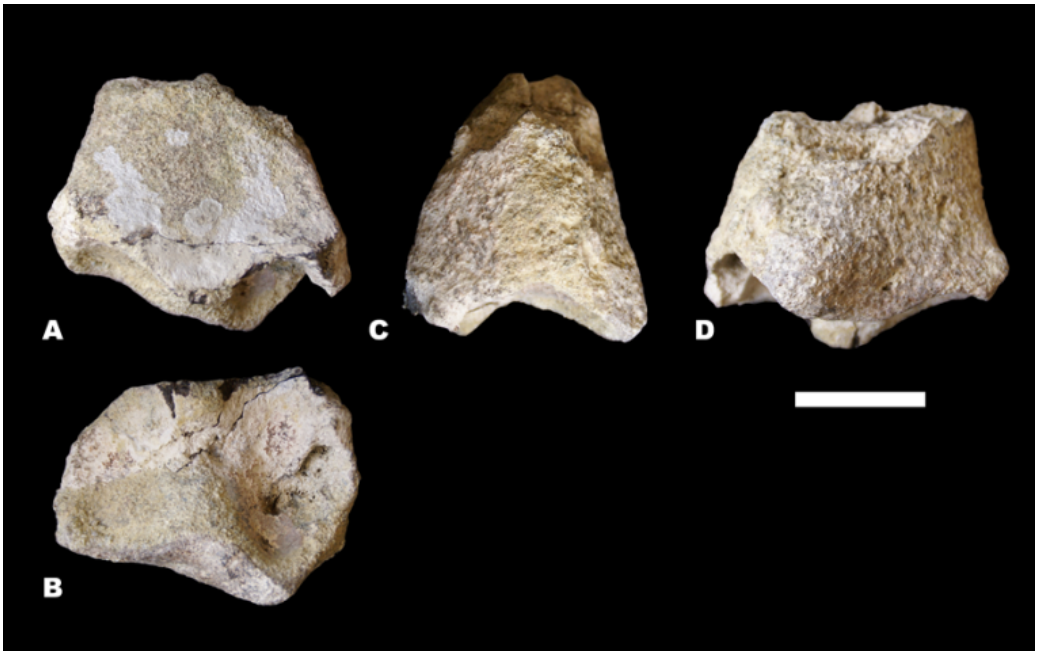

Supplementary Figure 4.6: Specimen #MW2-B878, distal right tibia of *H. gorgops*, fractured by percussion. A) anterior view; B) distal view; C) medial view; D) posterior view. Scale bar: 5 cm.

Description: Dentition: The left lower canine is a typical curved large tooth with half-moon section, probably corresponding to a male. The first premolar has only one root and the crown is partially destroyed. Also, it was not possible to study the upper canine and the juvenile mandible. The lower central incisor #MW5-B135 is a cylindrical tooth of large size, slightly curved to lingual face in the apex, with the apical region partially destroyed. The 2 germinal lobes of upper M3 #MW5-B66 are not fused, with the labial face destroyed. They show lingual and distal cingulum, and the mesial one is not preserved. It is not possible to take anatomical measurements. The upper left M1, which is poorly preserved, is very worn, and presents distal cingulum (Supplementary table 4.4).

Postcranial elements: The specimen #MW2-B929 is a bone fragment from a medial tibia region, with robust cortex. It was probably broken by percussion when fresh. The specimen #MW2-B878 is a distal end of robust right tibia, also probably broken by percussion when fresh (Supplementary Figure 4.6). The tibia fragment #MW2B929 shows a probable percussion mark in the proximal region, where it is thinner and more fragile (Figure 10, main text). This specimen probably corresponds to a single specimen , together with #MW2-B930 and #MW2-B878, all coming from the same horizon. The specimens #MW2-B932 and #MW2-B933 correspond to the right and left tali of a male and a female, respectively. The sexual dimorphism is well marked, with the male bone much larger than the female one (See Supplementary figure 4.5). The IV metatarsal from the MW4 falls within the typical range of variability of *Hippopotamus gorgops*.

Discussion: These specimens fall anatomically and metrically in the normal range of variability of the African early Pleistocene species *Hippopotamus gorgops* (aprox. 1.6 to 0.6 Ma), which is synonym of the European taxon *H. antiquus* ((Rook and Martínez-Navarro, 2010; Martínez-Navarro, 2010; Martínez-Navarro et al., 2015). Hippos are

the best represented large mammals at Melka Wakena. Combined with the presence of crocodiles, this means that the environment is dominated by abundant quantities of water in deep rivers or lakes.

Suborder Ruminantia Scopoli, 1777
Family Giraffidae Gray, 1821
Genus *Giraffa* Brisson, 1756
Species *Giraffa* cf. *jumae* Leakey, 1965

Material: #MW2-B620: Left lower premolar (p4), from the archaeological horizon MW2-L3.

Description: The only current record of a giraffid in the MW site is a dental piece from MW2-L3. It is a well-preserved left p4, although somewhat worn, with well-developed protoconid and metaconid, and prominent hypoconid and entoconid (Supplementary table 4.5 and Supplementary figure 4.7).

Supplementary Table 4.5. Measurements of the tooth of *Giraffa* cf. *jumae*

***Giraffa* cf. jumae,** *, left p4*		
	L	*W*
#MW2-B620	26.69	22.23

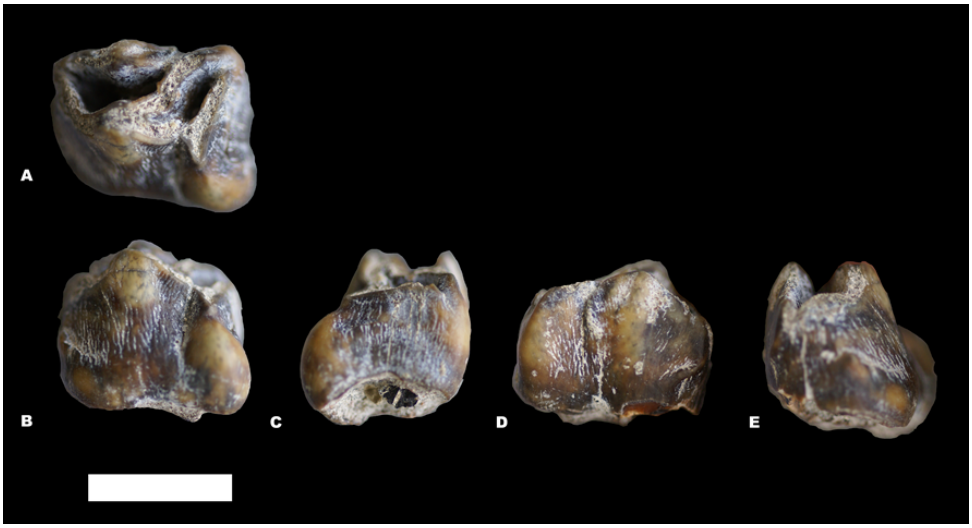

Supplementary Figure 4.7: Lower left P_4 of *Giraffa* cf. *jumae*. A) occlusal view; B) labial view; C) distal view; D) lingual view; and E) mesial view. Scale bar: 2 cm.

Discussion: The specimen's size and anatomy fall in the range of variability of *Giraffa jumai*, which is well recorded in the early and middle Pleistocene of eastern Africa, at Koobi Fora (Harris, 1991) and also cited at the site of Buia, Eritrea (Martínez-Navarro et al., 2004). It has similar size to the extant species *Giraffa camelopardalis*, cited at the site of 'Ubieidiya, Israel (Geraads, 1986) or at the early middle Pleistocene site of Asbole, Ethiopia (Geraads et al., 2004).

Family Bovidae Gray, 1821
Subfamily Bovinae Gray, 1821
Tribe Tragelaphini Blyth, 1863
Genus *Tragelaphus* (Blainville, 1816)
Species *Tragelaphus* sp. (small-middle size)

Material: Left upper M1 from MW5-L2b. (Supplementary Table 5.6, Supplementary figure 5.8).

Description: A brachyodont left upper M1, well-preserved in general but with the lingual wall destroyed in the protocone area. It has robust base in the protocone and the hypocone. Para, meso and metastyle well-marked. It shows a small entostyle in the base, between both lobes.

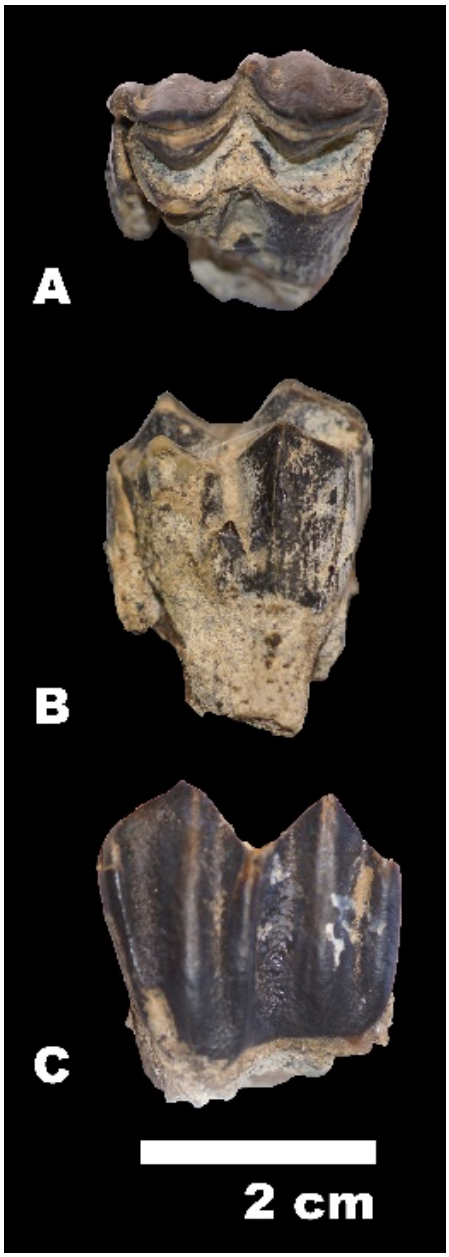

Supplementary Figure 4.8. Left upper M1 , MW5-L2b, ascribed to *Tragelaphus sp*. (small-middle size). A) occlusal view; B) lingual view; and C) labial view.

Discussion: This molar corresponds to a small-middle size brachydont bovid of the tribe Tragelaphini, which are the typical forest dwelling African antelopes. It falls in the size range of *Tragelaphus scriptus*, the extant harnessed bushbuck, which nowadays lives in forests of sub-Saharan Africa. It is impossible to tell if this could alternatively be a small size form related with sitatunga (*Tragelaphus spekei*) that is adapted to aquatic environments.

Supplementary Table 4.6. Measurements of the tooth ascribed to *Tragelaphus sp.* (small-middle size).

Tragelaphus sp., *left M1*			
	LWAL		*WPL*
n/n, MW5-L2b	*22.65*		*19.56*

Suborder Ruminantia Scopoli, 1777
Family Bovidae Gray, 1821
Subfamily Bovinae Gray, 1821
Tribe Bovini Gray, 1821
Genus indet. Cf. *Pelorovis* Reck, 1925
Species indet. Cf. *Pelorovis* sp.

Material: #MW5-B179, a distal metapodial trochlea from MW5-L2b.

Description: A distal metapodial trochlea with medio-lateral diameter of 31.64mm and dorso-ventral diameter of 35.72mm. The size corresponds to a buffalo, probably *Pelorovis*.

Discussion: This distal metapodial trochlea testifies the presence of a large buffalo, (probably *Pelorovis),* a typical inhabitant of open savannah environments, in the MW paleo-landscape.

Subfamily Antilopinae Gray, 1821
Tribe Antelopini Gray, 1821
Genus *Aepyceros* Sundevall, 1847
Species *Aepyceros* cf. *melampus* (Lichtenstein, 1812)

Material: right horncore from the MW4 area (N 0705134, E 3916325); left horncore from the MW8 area (N 0704815, E 3915657); #MW5-B163: rigth upper M1 (MW5L2a); #MW5-B158: right lower m1 (MW5-2b); #MW5-B157: right lower m2 (MW5L2b); #MW5-B44: left lower m2 (MW5-L2a); #MW5-B161: left lower p4 (MW5-L2a); #MW5-B188: right lower p4 (MW5 -L1); left lower m1 from MW5 sq L21 (MW5-L2a); #MW5-B136: left lower m1 (MW5-L2b); #MW5-B201: left lower molar fragment (MW5-L2b); #MW5-B152: lower m1-2 (MW5-L2b); #MW5-B98: lower m1-2 (MW5L2b); #MW5-B101 lower m1-2 (MW5-L2a); Left lower m1 from MW5 K21 no number (MW5-L2a).

Description: Horncores: Both specimens are stout with pneumatic pedicel. They are antelopes with elongated horncores and small torsion, heteronymous (right horncore with clockwise torsion) (Supplementary figure 4.9; Supplementary table 4.7).

Dentition*:* All the specimens correspond to a small-middle size antelope with very hypsodont teeth (Supplementary table 4.9). The upper M1 #MW5-B163 probably belongs to *A.* cf. *melampus,* well-preserved in general. The crown seems low because it is very worn. The labial wall of the metacone is destroyed. Proto, para, and hypocone are stout; the metacone is partially destroyed. It shows a pinched prefosseta and an enamel island between both fossetes.

The lower p4 MW5-B188 has a paraconid-metaconid junction, and the entoconid and entostylid are also fused. The lower molars show marked para, meso and metastylid, with rounded lobes in the labial face, and absence of ectostylid that is visible in the second lower molars #MW5-B44, #MW5-B157 (Supplementary figure 4.10).

***Supplementary Figure 4.9*:** left) right horncore found at MW4; right): left horncore from the area of MW8, corresponding to *Aepyceros* cf. *melampus*. Scale bar: 5 cm.

Supplementary Table 4.7: Measurements of the horncores specimens ascribed to *Aepiceros* cf. *melampus* from MW, compared with the data from Gentry and Gentry (1978a) for *A. melampus* from Olduvai.

Aepiceros* cf. *Melampus, horncores				
MW	*Total length*	*Circumfrerence. Base*	APD Base	MLD Base
MW5, left	*240*	*112*	*39.45*	*32.91*
MW4, right	*245*	*122*	*40.74*	*39.16*
OLDUVAI				
SHK II, surface BM(NH) M 26926			*35.7*	*29.3*
BK II , 1957.662			*36.8*	*31.3*

***Supplementary Table 4.8*:** Upper and lower dentition of *Aepyceros* cf. *melampus* from MW5.

***Aepyceros* cf. *melampus*,** *dentition*			
	L	WAL	WPL
#MW5-B163, right upper M1	*16.10*	*>12.77*	
#MW5-B158, right m1	*15.67*	*8.36.*	*9.36*
#MW5-B157, right, m2	*17.86*	*9.03*	*9.37*
#MW5-B44, m2	*17.44*	*9.90*	*10.54*
#MW5-B161, left p4	*12.58*	*7.51*	
#MW5-B188, right p4	*12.87*	*6.73*	

MW5 sq L21, left m1	*16.38*	*9.51*	*9.35 (very worn)*
#MW5- B136, left m1	*13.50*		*8.97*
#MW5- B201, left m frag.		*9.86*	
#MW5-B152, lower m1-2	*18.19*		*>8.55*
#MW5-B98, lower m1-2			*11.48*
#MW5-B101, lower m1-2			*11.25*
MW5 K21 n/n, Left lower m1		*9.04*	

Discussion: The comparison of this material with the Late Pleistocene impala from lake Victoria (Faith et al., 2014: Fig. 3), suggests that these specimens correspond to a primitive form of *Aepyceros melampus*.

The impalas (*Aepyceros*) are small-middle size antelopes. They are mixed feeders of grasses and leaves, that are common in open savanna habitats, but also in mixed woodlands. They are the best represented bovids at MW.

Supplementary Figure 4.10. #MW5- B157 right lower m2 of *Aepyceros* cf. *melampus*,. A) occlusal view; B) labial view; C) lingual view

Subfamily Antilopinae Gray, 1821
Tribe Antelopini Gray, 1821
Genus *Gazella* Blainville, 1816
Species *Gazella* sp.

Material: Right incomplete horncore (N 0705134, E 3916325) (MW4).

Description: A horncore with an oval section corresponding to the genus *Gazella*. Unfortunately, this single specimen does not allow a specific identification (Supplementary tabel 4.9; Supplementary figure 4.11).

Discussion: Gazelles are common grazing antelopes in east African savannahs.

Spplementary Table 4.9: Measurements of *Gazella sp*. horncore from MW4

***Gazella* sp.**, *horncore*		
MW4, right horncore	APD	MLD
base	*26.20*	*26.35*
5 cm base	*22.37*	*17.71*

Supplementary Figure 4 11. Right horncore of *Gazella* sp. from MW4. Scale 5 cm.

Species Antelopini indet.

Material: 1 lower right m2 (MW5-L2b); #MW5-B13: lower right m3 (MW5-L2a) (Supplementary figure 4.12; sup. Supplementary table 4.10).

Description: These specimens belong to a small-middle size species. The teeth are larger than those ascribed to *Aepyceros* cf. *melampus*.

The lower right m3 #MW5-B13 has rounded lobes in the protoconid and the hypoconid, and long hypoconulid, but the para, meta and entostylid are not well marked.

Supplementary Table 4.10. Second and third lower molars, ascribed to Antelopini indet.

Antelopini indt. cf., dentition			
	L	*WAL*	*WPL*
MW5-L2b n/n, lower right m2	*24.40*	*10.89*	*11.14*
#MW5-B13, lower right m3	*31.10*	*10.07*	*11.14*

Discussion: These fossils document the presence at MW of another grazing antelope species with hypsodont teeth After comparison with other sites (Gentry, 1985; 2010; Gentry and Gentry, 1978a and b), a specific taxonomic determination is not deemed possible.

Supplementary Figure 4.12. Lower rigth m3 B13 ascribed to Antelopini indet.

Subfamily Alcelaphinae Brook in Wallace 1876
Tribe Alcelaphini Brooke in Wallace, 1876
Species Alcelaphini indet.

Material: Right horncore and right upper M3 from the same outcrop (N 0704954, E 3915751), at MW3 area.

Description: Horncore: It is nearly complete, except for the posterior basal portion and the apical region, both destroyed. The specimen has pneumatic pedicel, it is compressed medio-laterally, and strongly curved backward at ~15 cm above the base, with some torsion from the base to the apex (Supplementary figure 4.13, Supplementary table 4.11).

Dentition: The upper right M^3 is an hypsodont tooth; the labial face of the anterior lobe and the base of labial face of the posterior lobe are destroyed. The enamel is thin. It has no entostyle and the labial styles are not well marked, especially the mesostyle. The metastyle is little prolonged to the distal region, especially in the base (Supplementary table 4.12).

Supplementary Table 4.11: Measurements of the horncore ascribed to Alcelaphini indet. (MW3).

Alcelaphini indet, *right horncore*				
	Preserved length	*Circumference at base*	*APD*	*MLD*
	275	*170*		
base			*62.64*	*43.97*
5 cm base			*51.61*	*46.48*
10 cm base			*48.15*	*43.80*
15 cm base			*40.74*	*39.18*

***Supplementary Figure 4.13*:** Right horncore from the area MW3 ascribed to Alcelaphini indet. Scale bar: 5 cm.

Discussion: Both specimens correspond to a middle size Alcelaphini antelope. These antelopes are the typical grazers in open savanna environments. With these few specimens it is not possible to classify the genus and the species. More material is necessary to be more concrete on the systematics of this species.

***Supplementary Table 4.12*:** Measurements of the dental specimen ascribed to Alcelaphini indet., from area of MW4.

Alcelaphini indet., dentition			

	L	*WAL*	*WPL*
MW3, right upper M3	*23.51*		*12.77*

General discussion and conclusions:

Biochronologically, all the fossil taxa can be ascribed to the second half of the early Pleistocene. The one exception is the lower third molar ascribed to *Elephas recki* cf. *brumpti,* an elephant chrono-subspecies with very primitive anatomical characteristics, known in eastern Africa from the Pliocene. At MW it is found in deposits post-dating 1.3 Ma. This anomaly is probably the outcome of reworking from earlier Pliocene sediments.

This faunal assemblage shows the abundance of some water-dependent species, especially the crocodile *Crocodylus* cf. *niloticus* and the mega-ungulate *Hippopotamus gorgops*. There are few species adapted to closed environments, such as *Tragelaphus* sp. (small-middle size), whereas additional taxa are more adapted to open savannah grassland, especially the antelope *Aepyceros* cf. *melampus*, Alcelaphini indet., Bovini indet. (Cf. *Pelorovis* sp.), but also *Metridichoerus modestus* or *Equus* sp. The presence of all this fauna together show the existence of mixed aquatic environments, savanna and forest.

Unfortunately, this faunal list is still short and sample sizes are small for any given taxon. Thus, temporal or ecological trends should be interpreted cautiously.

5. Lithic analysis

Primary data on the lithics was obtained using an attribute analysis (e.g., Isaac 1977). A series of characteristics (attributes) is documented for each artifact. For each attribute there are attribute states that represent the potential property (for qualitative attributes) or value (for quantitative attributes) the item may attain. For each specimen studied, any given attribute can be assigned a single attribute state. The selection of attributes is founded on published studies that applied the same technique to similar materials (Bar-Yosef and Goren-Inbar 1993:72) as well as on particular questions emerging during the study. Personal intuition and familiarity with the material play a role in the researcher's decisions about the attributes to be studied, with the lists of attributes and attribute states being continuously revised and re-evaluated. This dynamic nature of the analysis requires that attribute and

attribute states be listed explicitly. A principle of attribute analysis is that each artifact is described independently from others in the assemblage.

Thus, each artifact can be described by its typological, technological, and stylistic attributes, or by relationship among attributes. The observations can be quantified and relationship between attributes can be tested statistically.

The study of a lithic assemblage by attribute analysis in combination with the concept of reduction sequence enables quantification of observations pertaining to the physical state, metric and technological attributes of a large number of items (Bar-Yosef and Goren-Inbar 1993; Goren-Inbar 1990; Goren-Inbar et al. 2018; Hovers 1997, 1998, 2009; Isaac 1977; Tostevin 2000, 2011). The quantified information can be translated into sequential models that reconstruct the technological procedures. Because lithic reduction is a directional and irreversible process, these sequential models (e.g., Bleed 2001) yield a set of testable expectations from the initial phases until discard (e.g., Geneste 1985), providing a framework for reconstructing knapping behaviors. The relative sizes, shapes, amount of cortical cover, number of dorsal scars and other characteristics of the artifacts allow 'reverse engineering' of production methods. The stategies of technological organization of lithic production can be infered from "the patterning of the artifacts' properties" (Hovers 2007:54, 2009:19; for a formal application of this approach see Braun et al. 2008). Using an attribute analysis one can create a continuous feedback between the expected outcomes of the technical procedures observed upon the cores and core trimming elements (CTE) and the final products (Pelegrin 1990; Hovers 1997, 1998, 2009; Tostevin 2000). Such a dynamic approach mitigates some of the problems inherent to sequential models, including their potential 'stagnations' into a static typology of technology (e.g., Bar-Yosef and van Peer 2009).

MW cores were categorized following the classification applied by de la Torre (2011) for the study of the Gadeb assemblages (see Supplementary fig. 5.1 for a schematic representation and abbreviation of type names). De la Torre's schemes considered three technological procedures ('attributes'), each of which can attain variable attribute states:

1. *Interaction of knapping surfaces*: Cores can be classified into bifacial and unifacial exploitation systems. Unifacial reduction pertains to situations where flaking is restricted to a single surface, namely the reduction modes designated as USP,

UAU1, UAU2, UABI, UAUT, UP, and UC. Cores showing "frequent exchange of knapping surfaces", i.e., BSP, BAP, BALP, BALT, BP, BHC and Discoid methods belong in the bifacial exploitation systems (de la Torre 2011:775).

2. *Rotation of knapping surfaces:* During reduction cores are likely to be rotated for better grip and better flaking angles but not necessarily to the same degree. This variable of core reduction described full versus restricted rotation of the exploitation surface, and mainly relates to the length of exploitation series. UAUT, UABI, BALT, UP, BP, UC, BHC, and Discoid systems describe cores that show full rotation of knapping surfaces. USP, BSP, UAU1, UAU2, and BALP belong to a group manifesting restricted rotation of knapping surface, and hence shorter reduction series.
3. *Organization of core volume*: This aspect pertains to the management of the central volume of core in the knapping process- structured versus unstructured reduction sequences (de la Torre 2011). Most of the reduction modes above show exploitation restricted to the peripheral areas of the cores, without an effective exploitation of the central volume of cores. Discoid and BHC are typical examples of well-structured and successful exploitation of the central volumes of the cores. Multifacial and Polyhedral exploitation systems categorize cores exhibiting unstructured but successful maintenance of flaking surface(s).

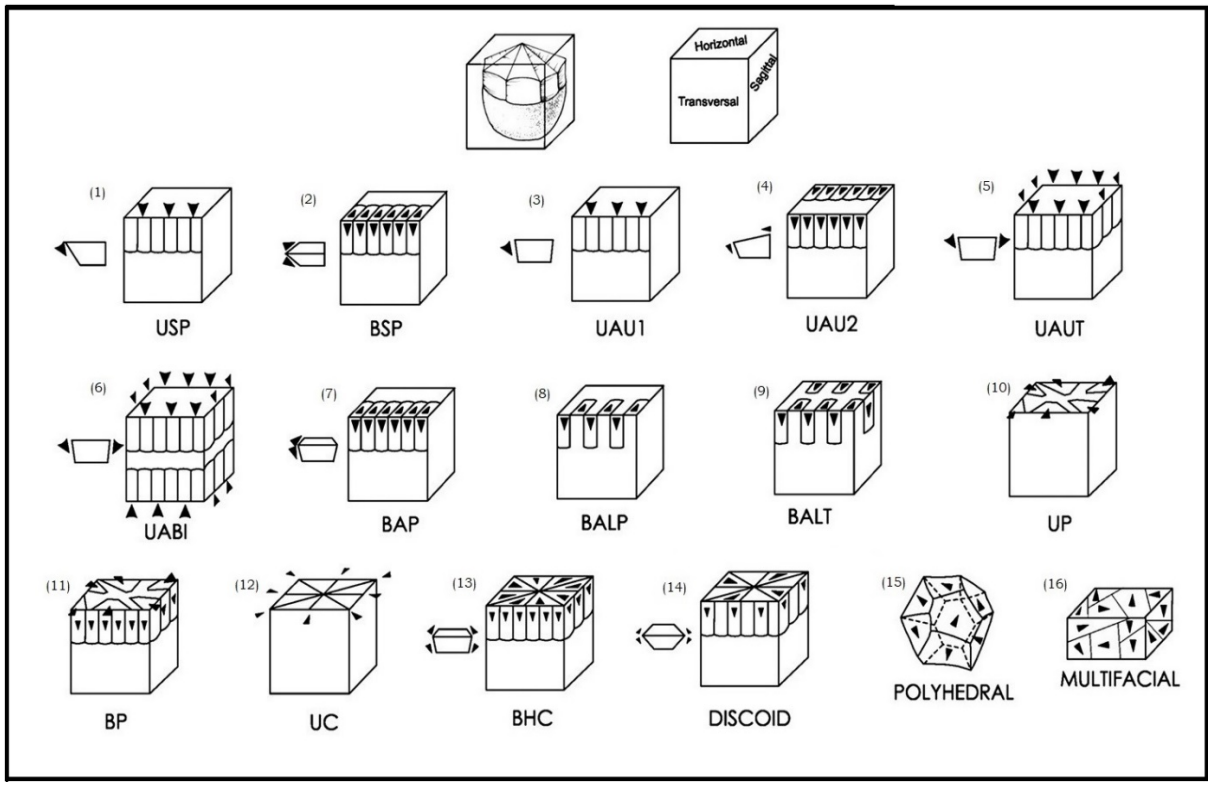

Supplementary figure 5.1: Hypothetical scheme of free-hand core reduction (modified from de la Torre, 2011; 1) USP: Unifacial simple partial exploitation. Flaking is unidirectional and restricted to one plane, from a natural striking platform and the angle between striking platform and the knapping surface is simple (<45º). 2) BSP: Bifacial simple partial exploitation. Flaking is unidirectional but in two adjacent surfaces, separated by a simple-angled bifacial edge. 3) UAU1: Unidirectional abrupt unifacial exploitation on one knapping surface. Flaking is unidirectional and limited to one surface, and the angle between the striking platform and the knapping surface is abrupt (>45º). 4) UAU2: Unidirectional abrupt unifacial exploitation on two independent knapping surfaces. Although there are two exploitation planes, there is no interaction between their respective striking platforms and knapping surfaces. Flaking is unidirectional, and the angle between striking platform and knapping surface is abrupt. 5) UAUT: Unifacial abrupt unidirectional total exploitation. There is only one striking platform, an abrupt angle of interaction between the striking and knapping surfaces, and flaking takes place all over transversal and sagittal planes of the core. 6) UABI: Unifacial abrupt bidirectional exploitation. Two opposed striking platforms are used to flake the same knapping surface, but there is no interchange between the striking and the knapping surfaces. 7) BAP: Bifacial abrupt partial exploitation. Flaking takes place in two adjacent surfaces separated by an abrupt angle, and the volume is partially exploited. 8) BALP: Bifacial alternating partial exploitation. Two adjacent surfaces are partially knapped by means of alternate flaking, using scars on the knapping surface of one plane as the striking platform for obtaining flake on the other plane. 9) BALT: Bifacial alternating total exploitation. The whole circumference of the core is exploited following the same bifacial alternating strategy as in the previous method. 10) UP: Unifacial peripheral exploitation. The horizontal plane is exploited unifacially through the rotation of the transversal and sagittal planes, but extractions do not meet in the center of the volume and reduction is limited to the edge of the core. 11) BP: Bifacial peripheral. Exploitation concentrates on the horizontal plane but there are two interactive surfaces, with the transversal and sagittal planes sometimes acting as preparation striking platforms for extractions on the horizontal plane. 12) UC: Unifacial centripetal exploitation. The horizontal plane is exploited unifacially through the rotation of the transversal and sagittal planes, and extractions are radial and usually meet towards the center of the knapping surface, facilitating the reduction of the volume. 13) BHC: Bifacial hierarchical centripetal. An

intersection plane divides the core into two asymmetrical and hierarchized volumes. Transversal and sagittal planes act as a subordinated volume (preparation surface) to obtain flakes in the main exploitation surface. 14) Discoid: this method is similar to BHC, except the unclear hierarchization of surfaces and the systematic alternating of strikes on the bifacial edge. 15) Polyhedral: cores with three or more knapping surfaces, which became spherical reduction sequence continued and covered the whole surface of the core. 16) Multifacial: cores with three or more knapping surfaces which show no clear organization of flaking but the irregular use of any available flaking angles.

In all the MW assemblages, variations of bifacial knapping methods were preferentially applied (MW2-L3, 52.7% [n=140]; MW2-L1&L2, 53.5% [n=23]; MW5-L1&L2, combined 70.7% [n=58]; MW1-S4&S3, combined 59.7% [n=41]). Their frequencies increase with time at the expense of reduction methods restricted to single surface of the core (MW2-L3 23.7%, [n=63]; MW5-L2&L1,9.8% [n=8]; MW1-S4&S3 13% [n=9]). Of the cores in the latter category, 66.7% (n=42) in MW2-L3, 83.3% (n=5) in MW2-L1&L2, 75% (n=6) in MW5-L2&L1, and 88.9% (n=8) in MW1-S4&S3 assemblages manifest extension of the core use lives, either by fully rotating the exploitation surface or by bidirectional knapping of the single surface.

Classification of the debitage followed of a number of influential studies (Andrefsky, 2005; Andrefsky and Andrefsky Jr, 1998; Goren-Inbar et al., 2018; Goren-Inbar and Sharon, 2006; Sullivan and Rozen, 1985), each of which focused on different morphological and technological aspects of the removed items. The category of complete flakes in this study includes both whole flakes as well as the minimally broken items if breakage does not affect the measurements of the flake dimensions (Sullivan and Rozen, 1985:759). Flakes with significant breakage on their margins that interferes or hinders accurate measurement of key dimensions are labelled as broken flakes (Sullivan and Rozen, 1985). Angular fragments (also sometimes known as core waste) do not bear discernible characteristics of a flake or any other defined knapping targets (Sullivan and Rozen, 1985; Andrefsky, 2005).

Metric measurements of flakes relate to their technological axis: length is the distance of the dorsal surface measured from the point of percussion on the proximal end to the distal tip, while width is the maximum dimension on a perpendicular axis to length (Andrefsky, 1998; 2005). On the basis of these metric parameters, whole

flakes were classified into large flakes and "intermediate" flakes (2-10 cm in length or width). Smaller detached items were recorded as microartifacts. The threshold of 10 cm for separating large flakes that were used as blanks for LCTs was suggested by Kleindienst (1961) and adopted by many later researchers (e.g., Baena Preysler et al., 2018; Beyene et al., 2013; Goren-Inbar et al., 2018; Leakey, 1971; Semaw et al., 2009; Sharon, 2007). Four types of flakes were recognized among the MW large flakes:

1. *Transversal (side-struck) flakes, with the longest axis perpendicular to the axis of* flaking (e.g., de la Torre and Mora, 2018; Diez-Martin et al., 2014; Petraglia et al., 1999; 2005; Presnyakova et al., 2015, 2018)
2. *Oblique (special side-struck*), where the axis of flaking is oriented obliquely to the longest axis of the resultant flake (de la Torre and Mora, 2018; DiezMartín et al., 2014; Madsen and Goren-Inbar, 2004; Petraglia et al., 1999; Presnyakova et al., 2015; 2018).
3. *Longitudinal (end-struck) flakes,* in which the longest axis is oriented in the direction of blow (e.g., Goren-Inbar et al. 2011, 2018; Leakey 1971).
4. *Kombewa flakes***,** formed when a massive flake is detached from a large (boulder) cores and used as a core from the ventral face of which another large flake is removed (Dauvois 1981; Owen 1938; Tixier and Turq, 1999). The resultant Kombewa flakes bear marks of two ventral faces and a biconvex profile suitable for modification into a bifacial tool with minimum retouch at the *façonnage* stage (Beyene et al., 2015; Goren-Inbar et al. 2011; Inizan et al., 1992; Sharon 2007).

The lithic assemblages of Melka Wakena fall within the range of variability of the Acheulian technocomplex, given the presence "large cutting tools" (LCTs). Of the three main types that Kleindienst (1962) identified as the marker of the Acheulian (handaxes, cleavers, and knives), the MW assemblages contain the former two. Common attributes of the LCTs are their relatively large size, the use of a bifacial flaking and the investment in imposition of form. The handaxe is considered the

hallmark of the Acheulian. It is "characterized by a cutting edge around the entire circumference of the tool or more rarely around the entire circumference of the tool with the exception of the butt... usually bilaterally symmetrical, and more-or-less biconvex in major and minor sections", although each of these traits and/or their combinations are highly variable (Kleindienst 1962: 85).

The cleaver is similar in many morphological aspects to the handaxe, a main difference being a broad and unretouched distal working edge. Kleindienst (1962:88) distinguished between bifacial cleavers and unifacial cleaver flakes. Morphologically they are characterized by "…worked butts and /or edges, and a bit at one end more-or-less perpendicular to the long axis of the tool." This tool also demonstrates substantial variability (Kleindienst 1962; Sharon 2007), partly due to different sets of criteria used in the definition. Here we follow Herzlinger and Goren-Inbar (2019, and references therein) who defined a cleaver as a bifacially shaped flake tool possessing an unretouched distal edge that is formed by an intersection between the two flat surfaces of the ventral and dorsal faces and must be wider than half of the tool's maximal width

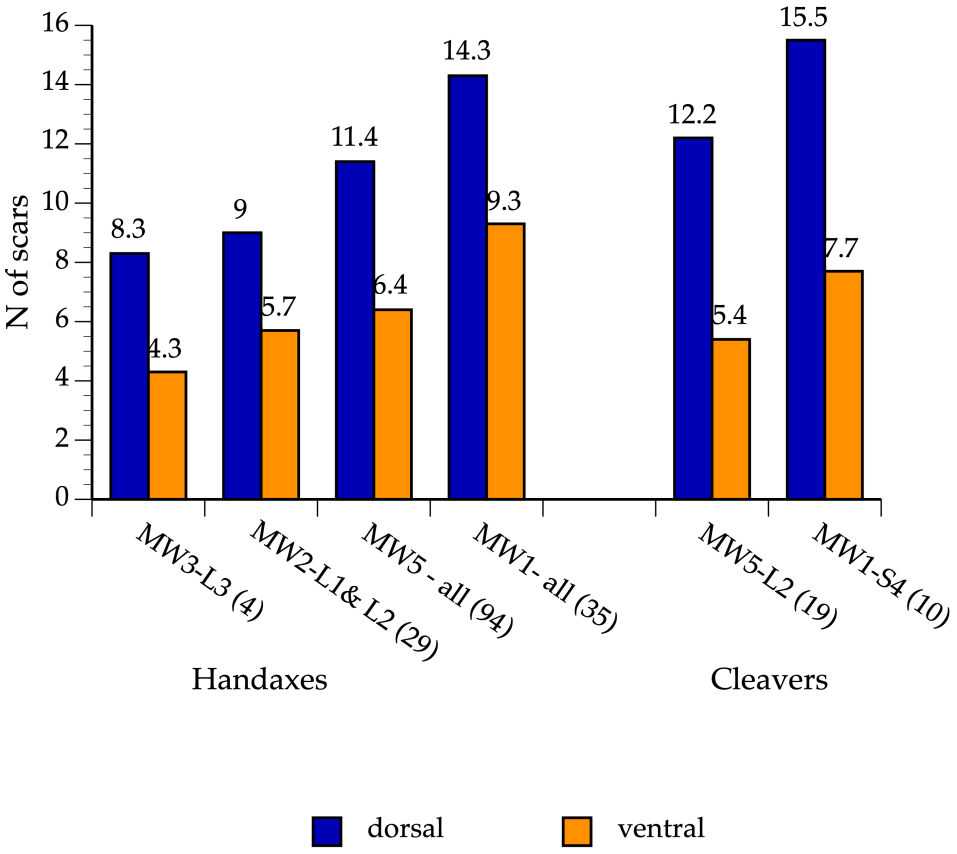

Supplementary figure 5.2: Average scar numbers (shown at the top of each column) on the dorsal and ventral faces of handaxes and cleavers from the *in situ* assemblages

References:

Andrefsky, W., 2005. Lithics: Macroscopic Approaches to Analysis. Cambridge University Press, Cambridge.

Andrefsky, W., Andrefsky Jr, W., 1998. Lithics. Cambridge University Press.

Baena Preysler, J., Torres Navas, C., Sharon, G., 2018. Life history of a large flake biface. Quaternary Science Reviews 190, 123-136. https://doi.org/10.1016/j.quascirev.2018.04.015

Bar-Yosef, O., Goren-Inbar, N., 1993. The Lithic Assemblages of 'Ubeidiya, a Lower Palaolithic Site in the Lower Jordan Valley. Institute of Archaeology, Jerusalem.

Bar-Yosef, O., Van Peer, P., 2009. The Chaîne Opératoire approach in Middle Paleolithic Archaeology. Curr. Anthropol. 50, 103-131.

Beyene, Y., Asfaw, B., Sano, K., Suwa, G., 2015. Konso Gardula Research Project. Volume 2: Archaeological Collections: Background and the Early Acheulian Assemblages. The University Museum, University of Tokyo

Beyene, Y., Katoh, S., WoldeGabriel, G., Hart, W.K., Uto, K., Sudo, M., Kondo, M., Hyodo, M., Renne, P.R., Suwa, G., Asfaw, B., 2013. The characteristics and chronology of the earliest Acheulean at Konso, Ethiopia. Proceedings of the National Academy of Sciences 110, 1584-1591. 10.1073/pnas.1221285110

Bleed, P., 2001. Trees or chains, links or branches: conceptual alternatives fo consideration of stone tool production and other sequential activities. Journal of Archaeological Method and Theory 18, 101-127.

Braun, D.R., Plummer, T., Ditchfield, P., Ferraro, J.V., Maina, D., Bishop, L.C., Potts, R., 2008a. Oldowan behavior and raw material transport: perspectives from the Kanjera Formation. J. Archaeol. Sci. 35, 2329-2345.

Braun, D.R., Rogers, M.J., Harris, J.W.K., Walker, S.J., 2008b. Landscape-scale variation in hominin tool use: evidence from the Developed Oldowan. J. Hum. Evol. 55, 10531063.

Churcher, C. S, Hooijer, D. A., 1980. The Olduvai Zebra (Equus Oldowayensis) from the Later Omo Beds, Ethiopia. Zoölogische mededelingen, ISSN 0024-0672, vol. 22, 21 pag., Ed. Rijksmuseum van natuurlijke historie (Leiden).

Dauvois, M., 1981. De la simultaneite des concepts Kombewa et Levallois dans l'Acheulieen du Maghreb et du Sahara nord-occidental, in: Roubet, C., Hagot, H.J., Souville, G. (Eds.), Préhistoire Africaine: Melanges offertsau doyen Lionel Balout. Editions A.D.P.E., Paris, pp. 313-321.

de la Torre, I., 2011. The Early Stone Age lithic assemblages of Gadeb (Ethiopia) and the Developed Oldowan/early Acheulean in East Africa. J. Hum. Evol. 60, 768-812. DOI: 10.1016/j.jhevol.2011.01.009

de la Torre, I., Mora, R., 2018. Technological behaviour in the early Acheulean of EF-HR (Olduvai Gorge, Tanzania). J. Hum. Evol. 120, 329-377. https://doi.org/10.1016/j.jhevol.2018.01.003

Diez-Martín, F., Sánchez Yustos, P., Gómez de la Rúa, D., Gómez González, J.Á., de Luque, L., Barba, R., 2014. Early Acheulean technology at Es2-Lepolosi (ancient MHSBayasi) in Peninj (Lake Natron, Tanzania). Quatern. Int. 322-323, 209-236. https://doi.org/10.1016/j.quaint.2013.08.053

Faith, J. T., Tryon, C. A., Peppe, D. J., Beverly, E. J., Blegen, N., 2014. Biogeographic and Evolutionary Implications of an Extinct Late Pleistocene Impala from the Lake Victoria Basin, Kenya. Journal of Mammalian Evolution 21, 213–222.

Ferretti, M. P., Ficcarelli, G., Libsekal, Y., Tecle, T. M., Rook, L., 2003. Fossil elephants from Buia (Northern Afar Depression, Eritrea) with remarks on the systematics of Elephas recki (Proboscidea, Elephantidae). Journal of Vertebrate Paleontology, 23, 244–257.

Gallotti, R., Mussi, M., 2017. Two Acheulians, two humankinds: from 1.5 to 0.85 at Melka Kunture (Upper Awash, Ethiopian Highlands).Journal of Anthropological Sciences 95, 137-181. doi 10.4436/JASS.95001

Geneste, J.-M., 1985. Analyse lithique d'industries moustériennes du Périgord: une approche technologique des comportements des groupes humains au Paléolithique moyen. Université de Bordeaux

Gentry, A. W., 1985. The Bovidae of the Omo group deposits, Ethiopia. In Y. Coppens et al. Eds. Les faunes Plio-Pléistocènes de la basse Vallée de l'Omo (Éthiopie). Cahiers Paléont., 1, 119-191.

Gentry, A. W., 2010. Bovidae. Chapter 38. In L. Werdelin and W. J. Sanders (Eds.) "Cenozoic Mammals of Africa". University of California Press, pp. 747-803.

Gentry, A. W., Gentry, A., 1978a. Fossil Bovidae (Mammalia) of Olduvai Gorge, Tanzania. Part I. Bull. Br. Mus. nat. Hist. (Geol.) 29 (4), 289-446.

Gentry, A. W., Gentry, A., 1978b. Fossil Bovidae (Mammalia) of Olduvai Gorge, Tanzania. Part II. Bull. Br. Mus. nat. Hist. (Geol.) 30 (1), 1-83.

Geraads, D., 1986. Les ruminants du Pléistocène d'Oubeidiyeh (Israël). In Tchernov, E. (Ed.) Les mammifères du Pléistocène inférieur de la Vallée du Jordain a Oubeidiyeh. Mem. Cen. Res. Franc. Jerusalem 5, 143-181.

Geraad, D., Alemseged, Z., Reed, D., Wynn, J. G., Roman, D. C., 2004. The Pleistocene fauna (other than Primates) from Asbole, lower Awash Valley, Ethiopia, and its environmental and biochronological implications. Geobios 37(6), 697-718.

Goren-Inbar, N., 1990. The Lithic Assemblages, in: Goren-Inbar, N. (Ed.), Quneitra – a Mousterian Site on the Golan Heights. Institute of Archaeology, Jerusalem, pp. 61167.

Goren-Inbar, N., Alperson-Afil, N., Sharon, G., Herzlinger, G., 2018. The Acheulian Site of Gesher Benot Ya'aqov, Vol. IV: The Lithic Assemblages. Springer, Cham.

Goren-Inbar, N., Grosman, L., Sharon, G., 2011. The technology and significance of the Acheulian giant cores of Gesher Benot Ya'aqov, Israel. J. Archaeol. Sci. 38, 1901-1917.

Goren-Inbar, N., Sharon, G., 2006. Invisible handaxes and visible Acheulian biface technology of Gesher Benot Ya'aqov, Israel, in: Goren-Inbar, N., Sharon, G. (Eds.), The Axe Age. Acheulian Tool Making from Quarry to Discard. Equinox Publishing, London, pp. 111-136.

Harris, J. M., 1991. Family Giraffidae. In J. M. Harris (ed.). Koobi Fora Research Project. Vol. 3, The Fossil Ungulates: Geology, Fossil Artiodactyls and Paleoenvironments, 93-138. Clarendon Press, Oxford.

Harris, J.M., White, T.D., 1979. Evolution of the Plio-Pleistocene African Suidae. Transactions of the American Philosophical Society 69, 1-128.

Herzlinger, G., Goren-Inbar, N., 2019. Beyond a cutting edge: a morpho-technological analysis of Acheulian handaxes and cleavers from Gesher Benot Ya'aqov, Israel. Journal of Paleolithic Archaeology. 10.1007/s41982-019-00033-5

Hovers, E., 1997. Variability of Lithic Assemblages and Settlement Patterns in the Levantine Middle Paleolithic: Implications for the Development of Human Behavior. The Hebrew University, Jerusalem

Hovers, E., 1998. The lithic assemblages of Amud Cave: implications for the end of the Mousterian in the Levant, in: Akazawa, T., Aoki, K., Bar-Yosef, O. (Eds.), Neandertals and Modern Humans in Southwest Asia. Plenum Press, New York, pp. 143-163.

Hovers, E., 2007. Book review of "Technological Strategies in the Lower Pleistocene at Olduvai Beds I and II" by Ignacio de la Torre and Rafael Mora. PaleoAnthropology 2007, 53-57.

Hovers, E., 2009. The Lithic Assemblages of Qafzeh Cave. Oxford University Press, New York.

Inizan, M.L., Roche, H., Tixier, J., 1992. Technology of Knapping Stone. CREP, Meudon.

Isaac, G.L., Isaac, B., 1977. Olorgesailie, Archaeological Studies of a Middle Pleistocene Lake Basin in Kenya. University of Chicago Press, Chicago.

Kleindienst, M.R., 1961. Variability within the Late Acheulian assemblage in East Africa. South African Archaeological Bulletin ARchaeolgolical Bullein 16, 35–52. doi:10.2307/3886868.

Kleindienst, M.R., 1962. Components of the East African acheulian assemblage: an analytic approach, in: Motelmans, C., Nenquin, J. (Eds.). Tervuren: Musée Royal de l'Afrique centrale, pp. 81-105.

Leakey, M.D., 1971. Olduvai Gorge Vol. 3, Excavations in Beds I and II, 1960-1963.

Cambridge University Press, Cambridge.

Lee, J.Y., Marti, K., Severinghaus, J.P., Kawamura, K., Yoo, H.S., Lee, J.B., Kim, J.S., 2006. A redetermination of the isotopic abundances of atmospheric Ar. Geochimica et Cosmochimica Acta 70, 4507-4512. 10.1016/j.gca.2006.06.1563

Lisiecki, L.E., Raymo, M.E., 2005. A Pliocene-Pleistocene stack of 57 globally distributed benthic δ 18O records. Paleoceanography 20. 10.1029/2004pa001071

Lister, A., 2015. Dating the arrival of straight-tusked elephant (Palaeoloxodon spp.) In Eurasia. Bull. Mus. Anthropol. préhist. Monaco, suppl. n° 6, 13-18.

Lordkipanidze, D., Jashashvili, T., Vekua, A., Ponce de León, M.S., Zollikofer, C.P.E., et al., 2008. Postcranial evidence from early Homo from Dmanisi, Georgia. Nature 449, 305310. doi:10.1038/nature06134

LordkipanidzeD., Ponce de León, M. S., Margvelashvili, A., Rak, Y., Rightmire, G. P., Vekua, A., Zollikofer, C. P. E., 2013. A Complete Skull from Dmanisi, Georgia, and the Evolutionary Biology of Early Homo. Science 342, 326-331.

Madsen, B., Goren-Inbar, N., 2004. Acheulian giant core technology and beyond: An archaeological and experimental case study. Eurasian Prehistory 2, 3-52.

Martínez-Navarro, B., 2010. Early Pleistocene faunas of Eurasia and hominid dispersals. In: Fleagle, J.G., Shea, J.J., Grine, F.E., Baden, A.L., Leakey, R.E. (Eds.), The First Hominin colonization of Eurasia, Contribution from the Second Stony Brook Human Evolution Symposium and Workshop, September 27-30, 2005, Springer, pp. 207e224 (Chapter 13).

Martínez-Navarro, B., 2016. Paleontological report: Preliminary study of the Vertebrate fauna from the Acheulian site of Melka Wakena (Ethiopia). Unpublished, *14pp.*

Martínez-Navarro, B., Madurell-Malapeira, J., Ros-Montoya, S., Espigares, M. P., Figueirido, B., Guerra-Merchán, A., Palmqvist, P., 2015. Sobre la paleobiología de Hippopotamus antiquus Desmarest, 1822: Un megaherbívoro acuático sin análogos vivientes?. In: M. Reolid Ed., Abstracts of the XXXI Jornadas de Paleontología. Sociedad Española de Paleontología, Baeza, Spain. Pp. 124-126. Martínez-Navarro, B., Rook, L., 2003. Gradual evolution in the African hunting dog lineage Systematic implications. CRPalevol 2, 695-702.

Martínez-Navarro, B., Rook, L., Segid, A., Yosieph, D., Ferretti, M.P., Shoshani, J., Tecle, T.M., Libsekal, Y., 2004. The large fossil mammals from Buia (Eritrea): systematics, biochronology and paleoenvironments. Riv. Ital. Paleontol. Stratigr. 110 (61–88, Supplement).

Niespolo, E.M., Rutte, D., Deino, A.L., Renne, P.R., 2017. Intercalibration and age of the Alder Creek sanidine 40Ar/39Ar standard. Quaternary Geochronology 39, 205-213. https://doi.org/10.1016/j.quageo.2016.09.004

Owen, W.E., 1938. The Kombewa culture, Kenya colony. Man 38, 203-205.

Pelegrin, J., 1990. Prehistoric lithic technology: some aspects of research. Archaeological Review from Cambridge 9, 116-125.

Petraglia, M., LaPorta, P., Paddayya, K., 1999. The first Acheulian quarry in India: stone tool manufacture, biface morphology, and behaviors. J. Anthropol. Res. 55, 39-70.

Presnyakova, D., Archer, W., Braun, D.R., Flear, W., 2015. Documenting differences between Early Stone Age flake production systems: An experimental model and archaeological verification. PLoS ONE 10, e0130732. 10.1371/journal.pone.0130732

Presnyakova, D., Braun, D.R., Conard, N.J., Feibel, C., Harris, J.W.K., Pop, C.M., Schlager, S., Archer, W., 2018. Site fragmentation, hominin mobility and LCT variability reflected in the early Acheulean record of the Okote Member, at Koobi Fora, Kenya. J. Hum. Evol. 125, 159-180. https://doi.org/10.1016/j.jhevol.2018.07.008

Renne, P.R., Cassata, W.S., Morgan, L.E., 2009. The isotopic composition of atmospheric argon and Ar-40/Ar-39 geochronology: Time for a change? Quaternary Geochronology 4, 288-298. 10.1016/j.quageo.2009.02.015.

Renne, P.R., Balco, G., Ludwig, K.R., Mundil, R., Min, K., 2011. Response to the comment by W.H. Schwarz et al. on " Joint determination of 40K decay constants and 40Ar */ 40K for the Fish Canyon sanidine standard, and improved accuracy for 40Ar/ 39Ar geochronology" by P.R. Renne et al. (2010). Geochim. Cosmochim. Acta 75, 50975100. https://doi.org/10.1016/j.gca.2011.06.021

Renne, P.R., Sprain, C.J., Richards, M.A., Self, S., Vanderkluysen, L., Pande, K., 2015. State shift in Deccan volcanism at the Cretaceous-Paleogene boundary, possibly induced by impact. Science (80-.). 350, 76–78. https://doi.org/10.1126/science.aac7549

Resom, A., Asrat, A., Gossa, T., Hovers, E., 2018. Petrogenesis and depositional history of felsic pyroclastic rocks from the Melka Wakena archaeological site-complex in South central Ethiopia. J. Afr. Earth Sci. 142, 93-111. https://doi.org/10.1016/j.jafrearsci.2018.03.003

Rook, L., Martínez-Navarro, B., 2010. Villafranchian: the long story of a Plio-Pleistocene European large mammal biochronologic unit. Quaternary International 219, 134-144.

Semaw, S., Rogers, M.J., Stout, D., 2009. The Oldowna-Acheulian transition: Is there a "Developed Oldowan" artifat traditions?, in: Camps, M., Chauhan, P. (Eds.), Sourcebook of Paleolithic Transitions. Springer Science +Business Media, New York, pp. 173-193.

Sharon, G., 2007. Acheulian Large Flake Industries: Technology, Chronology, and Significance. . Archaeopress, Oxford.

Sullivan, A.P., Rozen, K.C., 1985. Debitage analysis and archaeological interpretation. American Antiquity 50, 755-779.

Tixier, J., Turq, A., 1999. Kombewa et alii. Paléo 11, 135-143.

Tostevin, G.B., 2000. Behavioral Change and Regional Variation Across the Middle to Upper Paleolithic Transiton in Central Europe, Eastern Europe, and the Levant, Department of Anthropology. Harvard University, Cambridge MA